THE JOURNAL OF BIOLOGICAL CHEMISTRY VOL. 288, NO. 3, pp. 2040–2048, January 18, 2013

The Calmodulin Regulator Protein, PEP-19, Sensitizes ATP-induced Ca^{2+} Release*[S]

Received for publication, August 17, 2012, and in revised form, November 29, 2012 Published, JBC Papers in Press, November 30, 2012, DOI 10.1074/jbc.M112.411314

Xu Wang[‡], Liang Wen Xiong[‡], Amina El Ayadi[§], Darren Boehning[§], and John A. Putkey[‡1]

From the [‡]Department of Biochemistry and Molecular Biology and Structural Biology Imaging Center, University of Texas Medical School, Houston, Texas 77030 and the [§]Department of Neuroscience and Cell and Biology, University of Texas Medical Branch, Galveston, Texas 77555

Background: PEP-19 modulates the kinetics of Ca^{2+} binding to CaM.
Results: An acidic region in PEP-19 binds Ca^{2+} and is essential for both modulating Ca^{2+} binding to CaM and sensitizing cells to ATP-induced Ca^{2+} release.
Conclusion: Simply binding to CaM is not sufficient to account for the biological activities of PEP-19.
Significance: Regulating ligand-induced Ca^{2+} release gives PEP-19 the potential to broadly affect cell signaling.

PEP-19 is a small, intrinsically disordered protein that binds to the C-domain of calmodulin (CaM) via an IQ motif and tunes its Ca^{2+} binding properties via an acidic sequence. We show here that the acidic sequence of PEP-19 has intrinsic Ca^{2+} binding activity, which may modulate Ca^{2+} binding to CaM by stabilizing an initial Ca^{2+}-CaM complex or by electrostatically steering Ca^{2+} to and from CaM. Because PEP-19 is expressed in cells that exhibit highly active Ca^{2+} dynamics, we tested the hypothesis that it influences ligand-dependent Ca^{2+} release. We show that PEP-19 increases the sensitivity of HeLa cells to ATP-induced Ca^{2+} release to greatly increase the percentage of cells responding to sub-saturating doses of ATP and increases the frequency of Ca^{2+} oscillations. Mutations in the acidic sequence of PEP-19 that inhibit or prevent it from modulating Ca^{2+} binding to CaM greatly inhibit its effect on ATP-induced Ca^{2+} release. Thus, this cellular effect of PEP-19 does not depend simply on binding to CaM via the IQ motif but requires its acidic metal binding domain. Tuning the activities of Ca^{2+} mobilization pathways places PEP-19 at the top of CaM signaling cascades, with great potential to exert broad effects on downstream CaM targets, thus expanding the biological significance of this small regulator of CaM signaling.

PEP-19 (Purkinje cell protein 4, Pcp4) is a small protein (62 amino acids) with no known intrinsic activity other than binding to CaM[2] in the presence or absence of Ca^{2+}. Although it was originally identified in the central nervous system, PEP-19 mRNA is also found in human bladder, kidney, prostate, uterus, thyroid, and adrenal tissues (1). Changes in expression levels suggest biological roles for PEP-19 in both normal and pathological conditions. For example, PEP-19 mRNA levels are significantly reduced in a mouse model for Parkinson disease (2) and in the prefrontal cortex of alcoholics (3), but its levels are increased in anergic B cells (4) and in human uterine leiomyomas (5).

Animal and cellular model systems have demonstrated effects of PEP-19 on diverse cellular processes. PEP-19 null mice show a dramatic reduction in long term plasticity at synapses between granule cell parallel fibers and Purkinje cells (6). Overexpression of PEP-19 in PC12 cells increases neurite outgrowth (7), and premature neuronal differentiation is seen in transgenic mice with three copies of the PEP-19 gene (*Pcp4*) (8). The latter suggests a role for PEP-19 in Down syndrome because the human PEP-19 gene (*PCP4*) is present on chromosome 21. In addition, PEP-19 has anti-apoptotic activity when expressed in PC12 and HEK293T cells (9, 10), and it provides protection against Ca^{2+} overload in cortical neurons (10). These experimental observations are consistent with a proposed neuroprotective role for PEP-19 based on expression patterns in neuronal tissues that are susceptible to Huntington and Alzheimer diseases (11).

The above studies emphasize the need to understand the mechanism of action of PEP-19. Two models for PEP-19 have been proposed based on studies using peptides and the homologous proteins neurogranin (Ng) and neuromodulin (12–14). The first, or camstatin model, proposes that PEP-19 competitively inhibits activation of CaM target proteins. The second, or calpacitin model, proposes that PEP-19 binds with high affinity to apo-CaM to retard its release from PEP-19, thereby affecting the temporal profile of available CaM during a Ca^{2+} pulse. We proposed an alternative or additional mechanism for PEP-19 based on its ability to modulate the Ca^{2+} binding properties of CaM. Specifically, PEP-19 increases both the Ca^{2+} k_{on} and k_{off} rates at the C-domain of CaM up to 40-fold with little effect on the K_{Ca} (15). We also showed that an acidic sequence located adjacent to the IQ motif is required to modulate Ca^{2+} binding

* This work was supported, in whole or in part, by National Institutes of Health Grants GM081685 and GM081685-03S1 (to D. B.) and GM06961109 (to J. A. P.). This work was also supported by Fellowships R90 DK071504 from the W. M. Keck Center for Interdisciplinary Biosciences, 10POST3110010 from the American Heart Association (to X. W.), and GRNT2280427 from the American Heart Association (to J. A. P.).
[S] This article contains supplemental Fig. S1.
[1] To whom correspondence should be addressed: Dept. of Biochemistry and Molecular Biology and Structural Biology Imaging Center, University of Texas Health Medical School, 6431 Fannin St., Houston, TX. Tel.: 713-500-6061; Fax: 713-500-0652; E-mail: john.putkey@uth.tmc.edu.
[2] The abbreviations used are: CaM, calmodulin; C-CaM, isolated C domain of CaM; Ng, neurogranin; BAPTA, 1,2-bis(2-aminophenoxy)ethane-*N*,*N*,*N*′,*N*′-tetraacetic acid; IP_3, inositol 1,4,5-trisphosphate; CaM(DA) donor- and acceptor-labeled CaM.

to the C-domain of CaM, even though it has no apparent intrinsic affinity for CaM (16). Thus, the acidic/IQ motif of PEP-19 has the potential to modulate the rate-limiting kinetics of Ca^{2+} binding to CaM.

This study investigates the molecular mechanism by which PEP-19 modulates Ca^{2+} binding to CaM, and it tests the hypothesis that the biological activities of PEP-19 rely on synergy between the biochemical properties of its acidic and IQ sequences. Our results show that the acidic sequence in PEP-19 has intrinsic metal binding properties that play a role in increasing the rates of Ca^{2+} binding to CaM, at least in part, by electrostatically steering Ca^{2+} to and from Ca^{2+} binding sites III and/or IV. We also show that PEP-19 sensitizes HeLa cells to ATP-dependent Ca^{2+} release and that this effect is greatly reduced or eliminated by mutations in PEP-19 that inhibit or eliminate its ability to modulate Ca^{2+} binding to CaM. Tuning the activities of Ca^{2+} mobilization pathways by PEP-19 greatly expands the biological significance of this small regulator of CaM signaling.

EXPERIMENTAL PROCEDURES

Mutagenesis and Protein Purification—QuikChange II XL site-directed mutagenesis kit (Stratagene) was used to generate a panel of PEP-19 mutants. CaM and C-CaM (isolated C domain of calmodulin) were decalcified by addition of 5 mM EDTA and 0.1 mM BAPTA as a UV marker and then desalting on a Bio-Gel P2 column (Bio-Rad) in 10 mM NH_4HCO_3 that had been decalcified using a Ca^{2+} sponge column (Molecular Probes). Decalcified proteins were then lyophilized and resuspended in desired buffers. Protein concentrations were estimated using an extinction coefficient of $\epsilon_{276\ nm} = 0.18\ ml^{-1}\ mg^{-1}$ for C-CaM and $\epsilon_{215\ nm} = 0.59\ ml^{-1}\ mg^{-1}$ for PEP-19.

Ca^{2+} Binding Measurements—The rate of Ca^{2+} dissociation (k_{off}) from CaM or C-CaM in the presence or absence of PEP-19 derivatives was determined using stopped-flow fluorescence and the Ca^{2+}-sensitive dye Quin-2 as described previously (15). Typically, solutions of 2–5 μM CaM or C-CaM in 20 mM MOPS, pH 7.5, 100 mM KCl, 30 μM $CaCl_2$ were rapidly mixed with 20 mM MOPS, pH 7.5, 300 μM Quin-2. Excess free Ca^{2+} and Ca^{2+} that is rapidly released from the N-domain of CaM bind to Quin-2 in the 1.7-ms dead time of the stopped-flow instrument. The subsequent increase in Quin-2 fluorescence is due to binding Ca^{2+} released slowly from the C-domain. Experiments were performed at 23 °C using an Applied Photophysics Ltd. (Leatherhead, UK) model SX20 MV sequential stopped-flow spectrofluorimeter with a 150 watt Xe/Hg lamp.

Equilibrium Ca^{2+} binding constants for CaM in the presence or absence of PEP-19 derivatives were determined using tyrosine fluorescence at 23 °C as described previously (17). Data were collected with a QuantaMaster fluorimeter (Photo Technology International). Intrinsic Tyr emission spectra were recorded from 290 to 320 nm with the excitation wavelength of 276 nm. Solutions contained 20 mM MOPS, pH 7.5, 0 or 100 mM KCl, 1 mM EGTA, 1 mM HEDTA, 1 mM nitrilo-2,2′,2″-triacetic acid, 5 μM CaM or C-CaM with or without PEP-19 or its derivatives. Calcium was added from a concentrated stock prepared in the same buffer with CaM, PEP-19, and chelators, so that only the concentration of Ca^{2+} changes during the titration even though the volume increases. The concentration of total Ca^{2+} needed to achieve a desired free Ca^{2+} concentration was determined using the on-line calculator MaxChelator. Control titrations were performed using Br_2BAPTA as an indicator instead of CaM or C-CaM to confirm that the calculated free Ca^{2+} was accurate at high and low ionic strength. The K_{Ca} for Br_2BAPTA is 1.59 μM at 100 mM KCl and 0.15 μM at 10 mM KCl (18).

Tyrosine fluorescence intensity was plotted against the free Ca^{2+} concentration and fit to the following form of the Hill Equation 1,

$$F = F_{min} + (F_{max} - F_{min})\left[\frac{[Ca]^n}{[Ca]^n + [k_{Ca}]^n}\right] \quad \text{(Eq. 1)}$$

where $[Ca^{2+}]$ is the free Ca^{2+} concentration; F is the fluorescence intensity at a given free Ca^{2+} concentration; F_{min} is the initial fluorescence intensity in the absence of added Ca^{2+}; F_{max} is the fluorescence at maximal Ca^{2+}; K_{Ca} is the concentration of Ca^{2+} at which the change in fluorescence is half-maximal, and n is the Hill coefficient.

NMR Methodology—NMR experiments were performed on a Bruker DRX 600 MHz spectrometer equipped with a 5-mm triple resonance cryoprobe at 298 K. Protein samples were dissolved in buffer containing 10 mM imidazole, 5% D_2O (v/v), pH 6.3, 100 mM KCl. ^1H,^{15}N HSQC spectra were used to determine residues in PEP-19 that are affected by binding to C-CaM. Briefly, ^1H,^{15}N HSQC spectra were collected during titration of ^{15}N-labeled PEP-19 with C-CaM in the presence or absence of Ca^{2+}. Characteristics of fast exchange were seen at saturating Ca^{2+}, so backbone amides could be assigned by following cross-peaks during the titration. Slow exchange was seen in the apo-state, so assignments in the bound state were made using HNCO, HNCA, HN(CO)CA, HNCACB, CBCA(CO)NH, ^{15}N HSQC-TOCSY, and ^{15}N-edited NOESY-HSQC experiments. All NMR spectra were processed and analyzed using Topspin 2.0 (Bruker) and FELIX 2004 (MSI, San Diego). ^1H chemical shifts were referenced to 2,2-dimethyl-2-silapentane-5-sulfonate, and $^{15}N/^{13}C$ chemical shifts were referenced indirectly using their respective gyromagnetic ratios. The average amide chemical shift change was calculated using Equation 2,

$$\Delta\delta avg = \sqrt{\frac{(\Delta\delta H)^2 + (\Delta\delta N/5)^2}{2}} \quad \text{(Eq. 2)}$$

where $\Delta\delta H$ is the change in ^1H chemical shift and $\Delta\delta N$ is the change in ^{15}N chemical shift.

Calcium Imaging—Calcium imaging was performed exactly as described previously (19). HeLa cells were transfected with yellow fluorescent protein (YFP) only (control) or co-transfected with YFP and PEP-19 constructs at a DNA ratio of 1:4 using Lipofectamine 2000. Twenty four hours after transfection, single cell calcium responses evoked by NaATP were recorded from all YFP-positive cells in a given field. All experiments were repeated at least three times, and the data were pooled for statistical analysis. The actual number of single cell records averaged for each condition is indicated above the *bars* in Fig. 6*c*.

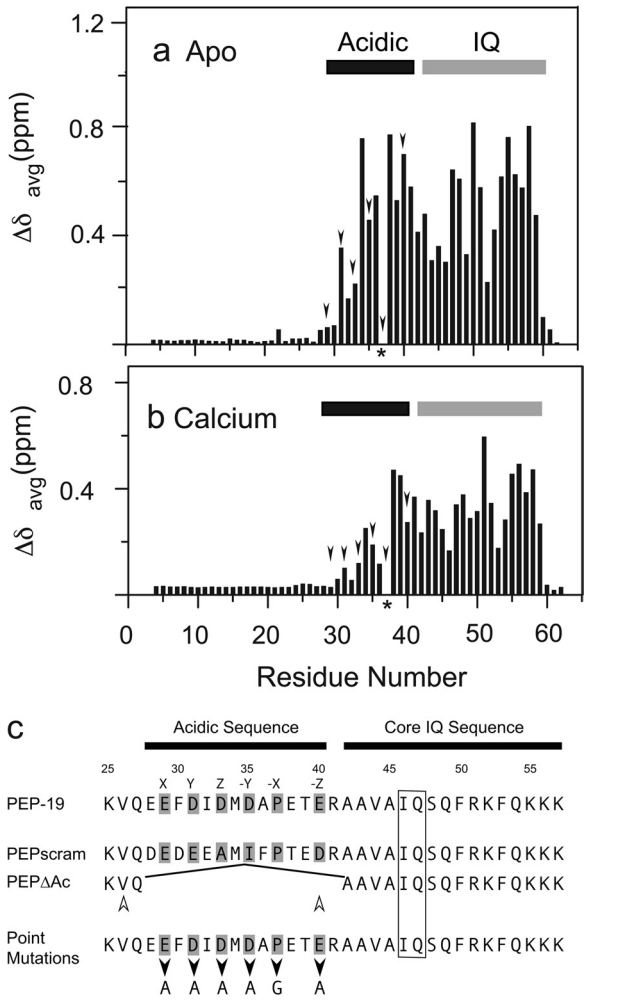

FIGURE 1. **Amide chemical shift changes in PEP-19 upon binding to C-CaM are restricted to the acidic/IQ region.** Average amide chemical shift perturbations were determined for residues in ^{15}N-labeled PEP-19 caused by binding to either apo (*a*) or Ca^{2+}-bound (*b*) C-CaM as described under "Experimental Procedures." The *arrowheads* indicate acidic residues that could potentially bind Ca^{2+}. The *asterisk* indicates Pro-37, which does not have a backbone amide. The core IQ sequence shown in *c* is based on comparison of multiple IQ motif proteins. Residues denoted by *X*, *Y*, *Z*, and $-Y$, $-X$, and $-Z$ in native PEP-19 correspond to potential Ca^{2+} ligand positions based on a canonical EF-hand Ca^{2+}-binding motif. PEPΔAc was generated by deletion of residues Glu-28 to Arg-41. The *open arrowheads* indicate that Val-26 is shifted to the position of Glu-40 in PEPΔAc. Residues 28–40 were randomly scrambled in PEPscram while retaining Pro-37. *Black arrowheads* indicate positions of point mutations.

RESULTS

PEP-19 Proteins Generated for Study—We used amide chemical shift perturbation to identify residues in PEP-19 that experience significant structural transitions upon binding to the C-domain of CaM because these residues will likely play key roles in regulating Ca^{2+} binding to CaM. C-CaM, which encodes residues 76–148 of CaM, was used for these experiments because we showed previously that PEP-19 binds to C-CaM and had the same effects on its Ca^{2+}-binding proteins as seen for full-length CaM (20). Fig. 1, *a* and *b,* shows that backbone amide chemical shifts for residues 1–30 in PEP-19 are unchanged upon binding to C-CaM in the absence or presence of Ca^{2+}. Because free PEP-19 is intrinsically disordered (21), these data show that residues 1–30 remain disordered when bound to C-CaM. Amide chemical shift perturbations are restricted to residues in the acidic/IQ region of PEP-19 upon binding to either apo- or Ca^{2+}-C-CaM.

Based on the above chemical shift perturbations, two sets of proteins were generated to test the biochemical and functional significance of the acidic sequence in PEP-19 (see Fig. 1*c*). The acidic sequence is deleted in PEPΔAc such that Val-26 effectively substitutes for Glu-40 of native PEP-19. We anticipated that a hydrophobic residue at this position would promote association of PEPΔAc with both the N- and C-domains of CaM because a Phe residue at the homologous position in the $Ca_V1.2$ channel anchors its IQ region to the N-domain (22). Residues in the acidic sequence of PEPscram are randomized to determine whether the native sequence is important for modulating Ca^{2+} binding to CaM or whether a cluster of negative charges is sufficient.

The second set of proteins was designed to test the functional significance of sequence similarity between the acidic region of PEP-19 and the consensus EF-hand Ca^{2+}-binding site where alternating residues provide oxygens to coordinate Ca^{2+} at *X*, *Y*, *Z* and $-Y$, $-X$, and $-Z$ positions (see Fig. 1*c*). Thus, Ala was substituted individually for Glu-29, Asp-31, Asp-33, Asp-35, or Glu-40. In addition, Pro-37 was changed to Gly to test the hypothesis that backbone constraints imposed by the cyclized Pro side chain dictates the relative positions of adjacent acidic residues when PEP-19 is bound to CaM, thereby affecting Ca^{2+} binding.

Deletion of the Acidic Sequence Prevents Modulation of Ca^{2+} Binding to CaM—Calcium-dependent Tyr fluorescence was used to measure the K_{Ca} of the C-domain of CaM in the presence or absence of native and mutated PEP-19. Table 1 shows that neither native PEP-19 nor its mutated derivatives have large effects on K_{Ca}, although most decreased the cooperativity of Ca^{2+} binding.

The relatively slow Ca^{2+} k_{off} rate of 10.4 s^{-1} for free CaM in Table 1 is due to dissociation of 2 Ca^{2+} from the C-domain because dissociation of Ca^{2+} from the N-domain is very rapid and occurs in the dead-time (1.7 ms) of the stopped-flow fluorimeter. PEP-19 greatly increases the rate of Ca^{2+} dissociation to about 300 s^{-1}, but the stoichiometry remains 2 Ca^{2+} released per CaM. Table 1 shows that deletion of the acidic sequence in PEPΔAc prevents the increase in Ca^{2+} k_{off}. Thus, the acidic sequence of PEP-19 is required for modulation of Ca^{2+} binding to CaM.

Interestingly, the stoichiometry of Ca^{2+} release in the presence of PEPΔAc is 4 Ca^{2+}/mol of CaM instead of 2 seen the presence of all other PEP-19 proteins. This is consistent with the above prediction that PEPΔAc binds to both the N- and C-domains of CaM, thereby slowing the rate of release of Ca^{2+} from the N-domain as is seen for other CaM-binding proteins and peptides (23). We confirmed this mode of binding using a donor- and acceptor-labeled CaM (CaM(DA)) (24), which gives a large decrease in fluorescence due to FRET when CaM adopts a compact structure upon binding both domains to one peptide. Fig. 2 shows that fluorescence from CaM(DA) is not greatly affected by native PEP-19 because it binds preferentially to the C-domain of CaM, but a large decrease in fluorescence is seen upon binding to either PEPΔAc or a CaM-binding peptide

TABLE 1

Effect of mutants on Ca^{2+} binding to CaM

Apparent K_{Ca} values were determined by monitoring Tyr fluorescence during titration with Ca^{2+} and fitting the data to the Hill equation as described under "Experimental Procedures." ND indicates not determined. Calcium dissociation rates (k_{off}) were derived by fitting Ca^{2+} dissociation curves to mono- or diexponential equations. Values for k_{off} are the average of 3–5 determinations in the presence or absence of 20 μM PEP-19 proteins. Stoichiometry of Ca^{2+} release was determined by calibrating Quin-2 fluorescence. Rates of Ca^{2+} association (k_{on}) were calculated from $k_{on} = k_{off}/K_{Ca}$.

	Equilibrium Ca^{2+} binding		Binding kinetics			Stoichiometry
PEP-19 protein	K_{Ca}	Hill coefficient	$k_{off,1}$	$k_{off,2}$	k_{on}	Ca^{2+}/protein
	μM		s^{-1}	s^{-1}	$s^{-1}\ \mu M^{-1}$	
None	1.6 ± 0.1	1.8 ± 0.1	10.4 ± 0.2		6.5	2.0
PEP-19	2.0 ± 0.1	1.1 ± 0.01	298 ± 10		149	1.8
mycPEP-19	2.0 ± 0.2	1.3 ± 0.04	303 ± 15		151	1.8
PEPΔAc	ND	ND	11.7 ± 0.6	36 ± 4	ND	1.7
PEPscram	1.9 ± 0.2	1.6 ± 0.05	10.6 ± 0.4		5.7	2.0
PEP(E29A)	2.3 ± 0.1	1.1 ± 0.03	276 ± 11		120	1.8
PEP(D31A)	2.4 ± 0.1	1.1 ± 0.01	157 ± 5		65	1.7
PEP(D33A)	1.6 ± 0.1	1.4 ± 0.04	94 ± 6		59	1.8
PEP(D35A)	2.4 ± 0.1	1.1 ± 0.1	288 ± 12		120	1.8
PEP(P37G)	1.6 ± 0.2	1.5 ± 0.02	69 ± 5		43	1.9
PEP(E40A)	2.4 ± 0.2	1.1 ± 0.03	159 ± 8		66	1.7

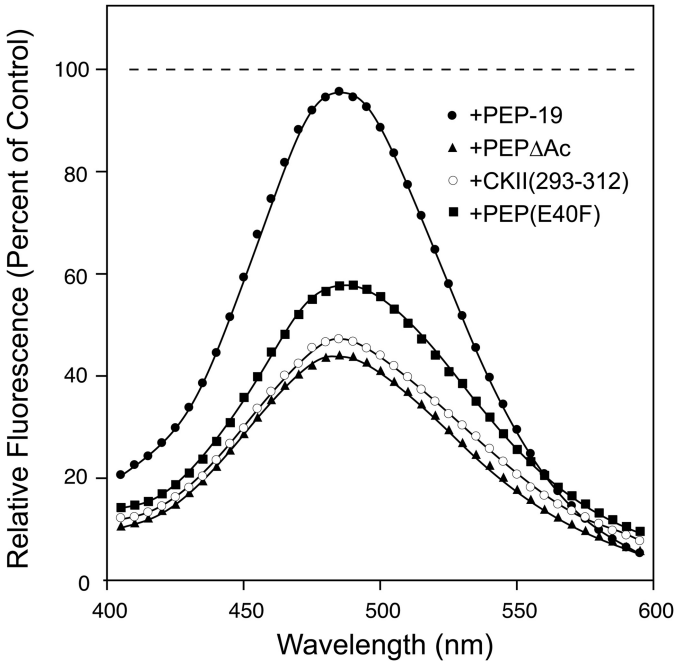

FIGURE 2. **PEPΔAc binds to both domains of CaM to induce a compact structure.** CaM(DA) has Thr-38 (N-domain) and Thr-110 (C-domain) converted to Cys and is labeled with a sulfhydryl-specific fluorescent donor (5-((((2-iodoacetyl)amino)ethyl)amino)naphthalene-1-sulfonic acid) and the nonfluorescent acceptor (*N*-(4-dimethylamino-3,5-dinitrophenyl)maleimide). The *dashed line* indicates the fluorescence maximum if no FRET effect was observed.

from CaM kinase II, CKII(293–312), which is known to bind to both domains of CaM (25). As a further test, we generated PEP(E40F), with Phe at the homologous position to the Phe that anchors the IQ motif of the $Ca_V1.2$ channel to the N-domain of CaM (22). Fig. 2 shows that PEP(E40F) also causes a large decrease in fluorescence upon binding to CaM(DA). These results show that the absence of an appropriately positioned hydrophobic group in the acidic region of PEP-19 allows preferential binding to the C-domain of CaM.

Native Sequence of the Acidic Region Is Necessary to Modulate Ca^{2+} Binding to CaM—Table 1 shows that PEPscram has essentially no effect on K_{Ca}, k_{off}, k_{on}, or the stoichiometry of Ca^{2+} binding to CaM. This lack of effect was so striking that we used NMR to determine whether PEPscram binds to CaM with the same domain specificity and exchange properties as native PEP-19. We showed previously that native PEP-19 binds to apo-CaM and Ca^{2+}-CaM with characteristics of slow and fast exchange, respectively, on the NMR time scale (21). Fig. 3 shows that PEPscram retains these properties. Specifically, Fig. 3*a* shows that PEPscram binds to apo-CaM with slow to intermediate exchange on the NMR time scale, causing severe broadening of backbone amide cross-peaks for residues in the C-domain, but it has little effect on amides in the N-domain (full spectra are supplied as supplemental material). Fig. 3*b* shows that PEPscram also selectively binds to the C-domain of Ca^{2+}-CaM, but with characteristics of fast exchange. Thus, both PEPscram and PEP-19 bind to the C-domain of apo- or Ca^{2+}-CaM, and with similar exchange characteristics, but PEPscram is incapable of modulating the Ca^{2+} binding properties of CaM.

None of the PEP-19 point mutations had significant effects on K_{Ca} of CaM, but Table 1 and Fig. 4*a* show that they have varying effects on k_{off} and k_{on}. Conversion of Glu-29 to Ala at the putative *X* coordination position had no effect. Mutation of Asp-31, Asp-33, or Glu-40 to Ala inhibited the ability of PEP-19 to increase k_{off} but to different extents. The properties of PEP(D35A) are very similar to native PEP-19, even though Asp-35 at the putative $-Y$ coordination position is centered between residues 31, 33, and 40. This could be explained by the fact that the $-Y$ position is highly variable in canonical EF-hand Ca^{2+}-binding loops because the backbone carbonyl oxygen, not the side chain, of this residue coordinates Ca^{2+}.

Fig. 4*b* shows that conversion of Pro-37 to Gly significantly decreased the ability of PEP-19 to modulate Ca^{2+} binding to CaM, although not to the extent seen for PEPscram. This suggests that backbone constraints imposed by the imide side chain of Pro-37 positions acidic residues in PEP-19 such that they can properly modulate Ca^{2+} binding to CaM. Therefore, mutation of Pro would be equivalent to mutating multiple acidic residues. This is consistent with the fact that PEPscram is incapable of modulating Ca^{2+} binding to CaM because it effectively has multiple acidic mutations.

Acidic Region of PEP-19 Binds Ca^{2+}—The distribution of acidic residues in PEP-19 led us to determine whether the acidic sequence has intrinsic Ca^{2+} binding activity. Its similar ionic

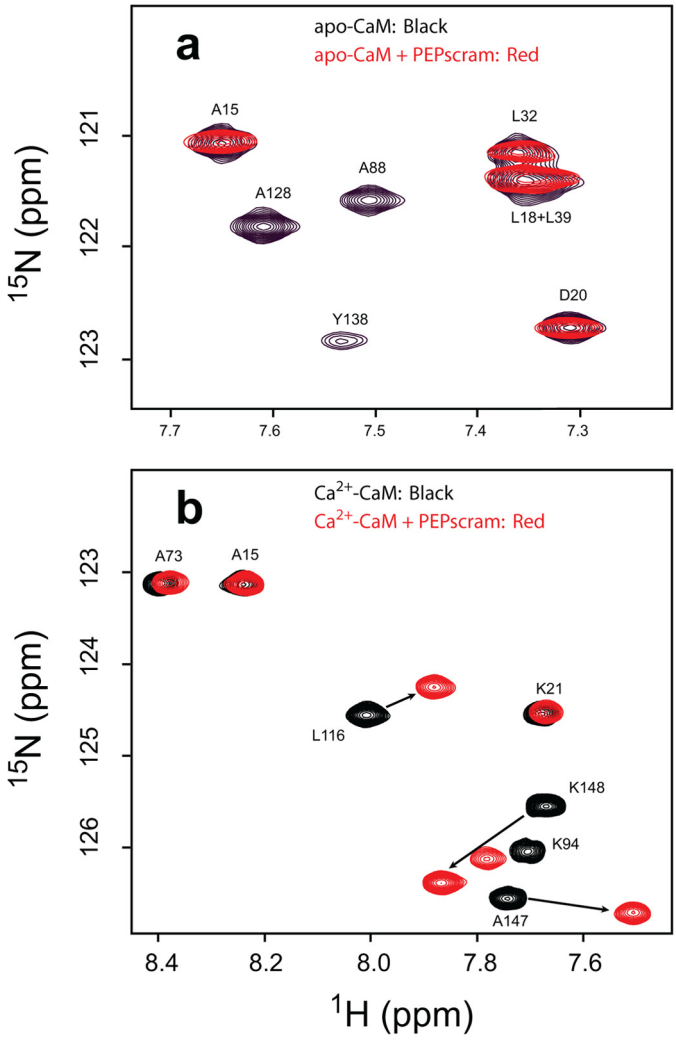

FIGURE 3. **^{1}H,^{15}N HSQC NMR spectra indicate binding of PEPscram to apo- and Ca^{2+}-CaM.** *a* shows a selected region of the overlaid ^{1}H,^{15}N HSQC spectra of apo-CaM (*black*) and apo-CaM in complex with PEPscram (*red*); *b* shows a selected region of the overlaid ^{1}H,^{15}N HSQC spectra of Ca^{2+}-CaM (*black*) and Ca^{2+}-CaM in complex with PEPscram (*red*). PEPscram binding causes amide resonances in Ca^{2+}-CaM undergoing fast exchange on the NMR time scale. The *arrows* in *b* highlight the movements of amide resonances in Ca^{2+}-CaM due to PEPscram binding.

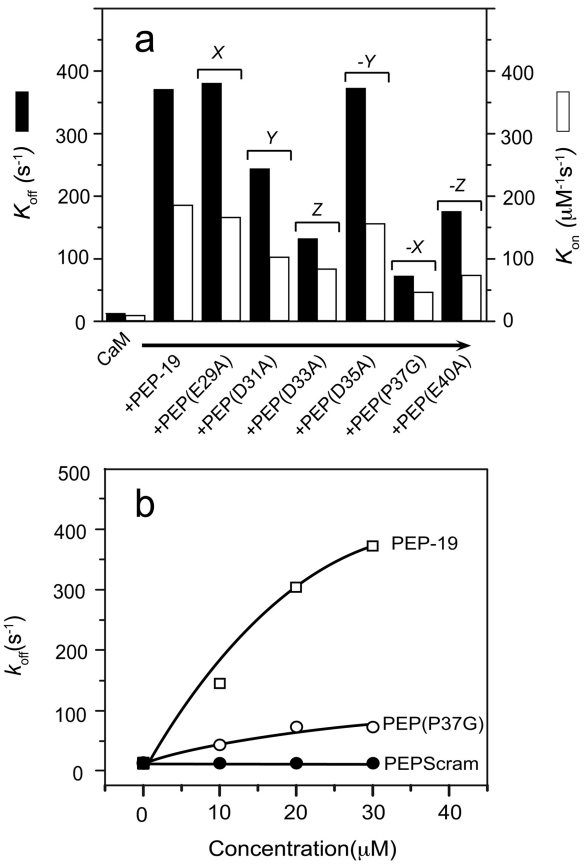

FIGURE 4. **Contribution of acidic residues in PEP-19 to modulating Ca^{2+} binding to the C-domain of CaM.** *a* shows the effects of specific acidic residues in PEP-19 on the rates of Ca^{2+} dissociation (*black bars*) and association (*white bars*) at the C-domain of CaM. Dissociation of Ca^{2+} was measured in the presence of 30 μM PEP-19 or the indicated mutant PEP-19. Dissociation rates are the average of 4–5 determinations. Association rates were calculated from k_{off} and K_{Ca} by $k_{on} = k_{off}/K_{Ca}$ (see Table 1). *b* shows the effect of increasing concentrations of PEP-19, PEP(P37G), and PEPscram on the rate of Ca^{2+} dissociation.

radii and metal coordination geometries to Ca^{2+} make paramagnetic Tb^{3+} a sensitive probe for identifying Ca^{2+}-binding sites (26). Fig. 5*a* shows that Tb^{3+} broadens backbone amide chemical shifts for residues in the acidic sequence of PEP-19, especially residues 31–36, which are severely broadened at a Tb^{3+}/PEP-19 ratio of 1:50. Amides for Asp-33 and Asp-35 are most affected and are broadened beyond detection at a Tb^{3+}/PEP-19 ratio of 1:100. These spectral perturbations indicate that Tb^{3+} binds to the acidic region in PEP-19.

Although Ca^{2+} is not paramagnetic, we reasoned that it might affect specific amide resonance intensities due to exchange broadening if Ca^{2+} binds to PEP-19. Indeed, Fig. 5*b* shows that addition of Ca^{2+} to PEP-19 causes exchange broadening of amide resonances in the acidic sequence relative to other regions in PEP-19. Similar to the effect of Tb^{3+}, Asp-33 and Asp-35 are most affected by addition of Ca^{2+} and show maximal broadening at a Ca^{2+}:PEP-19 molar ratio between 1 and 2 as shown in Fig. 5*c* with Arg-4 in the N-domain of CaM as a control. These spectral perturbations indicate that Ca^{2+} binds weakly to the acidic sequence of PEP-19.

Effect of Electrostatics on Ca^{2+} Binding—We reasoned that the acidic sequence of PEP-19 with intrinsic Ca^{2+} binding properties may increase the Ca^{2+} k_{on} if positioned near site III and/or IV of CaM by attracting or electrostatically steering Ca^{2+} to these binding sites. Because the contribution of electrostatic interactions would be decreased by monovalent cations, we predicted that decreasing the KCl concentration would increase the k_{on} for Ca^{2+} binding to the C-domain of CaM in the presence or absence of PEP-19. Table 2 shows the K_{Ca}, k_{off}, and k_{on} values for Ca^{2+} binding to the C-domain of CaM with or without 100 mM KCl and with or without 30 μM PEP-19. The Ca^{2+} binding affinity is increased about 13-fold at low ionic strength due primarily to a large increase in k_{on}. The effect of KCl on k_{on} can be explained by electrostatic shielding of acidic side chains on CaM that coordinate or attract Ca^{2+}. PEP-19 increases Ca^{2+} k_{on} by 27- and 45-fold at 100 and 0 mM KCl, respectively. This effect of PEP-19 can be attributed, at least in part, to electrostatic steering of Ca^{2+} ions via weak Ca^{2+} binding activity of the acidic sequence in PEP-19.

PEP-19 Sensitizes HeLa Cells to ATP-induced Ca^{2+} Release—ATP-induced Ca^{2+} release in HeLa cells was selected as an

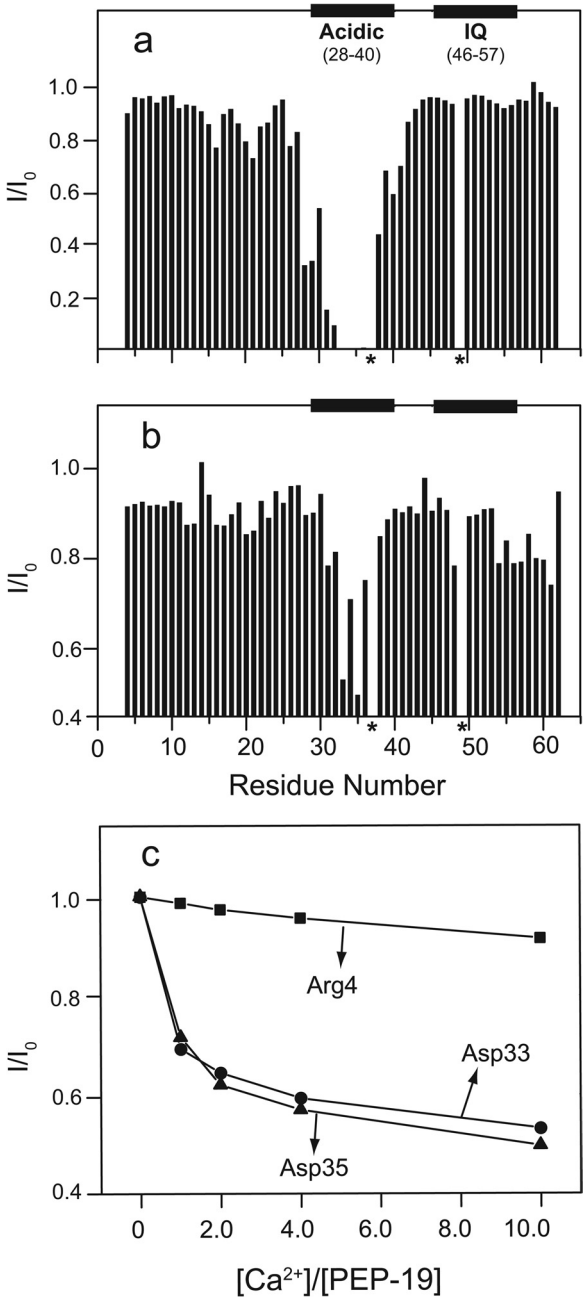

FIGURE 5. **Interactions between PEP-19 and metal ions monitored by $^{1}H,^{15}N$ HSQC spectra.** I/I_0 is the intensity ratio for backbone amide cross-peaks in the $^{1}H,^{15}N$ HSQC spectra of 0.5 mM PEP-19 collected in the presence (I) and absence (I_0) of 10 μM Tb^{3+} (*a*) or 5 mM Ca^{2+} (*b*) in the absence of KCl. *Panel c* shows the effect of increasing Ca^{2+} on I/I_0 for Asp-33 and Asp-35 relative to Arg-4, which is unaffected by specific binding of Ca^{2+}. * indicate the absence of backbone amides for Pro-37 and Gln-49, which could not be assigned.

initial model system to determine whether PEP-19 can impact a Ca^{2+} release pathway because this pathway involves multiple potential points of regulation by CaM, including P2Y G-protein-coupled receptors, phospholipase C, and the IP_3 receptor. PEPscram, PEP(P37G), and PEPΔAc were selected to test the biological significance of the acidic sequence because they all bind to CaM but have little or no effect on its Ca^{2+} binding properties. Expression plasmids for native and mutated PEP-19 were engineered with N-terminal Myc tags to readily determine relative expression levels in transfected cells. We anticipated that the Myc tag would not affect interactions between PEP-19 and CaM because residues 1–23 in PEP-19 are disordered when bound to CaM. As shown in Table 1, PEP-19 and mycPEP-19 have essentially identical effects on Ca^{2+} binding to CaM.

HeLa cells were transfected with a control YFP plasmid or cotransfected with YFP and PEP-19 plasmids at a 1:4 ratio. YFP-positive cells from different coverslips were selected for analysis. The Western blot in Fig. 6*a* shows comparable levels of expression of PEP-19 proteins in transfected cells, and it confirms that the apparent molecular mass of PEPΔAc is smaller than the other proteins due to deletion of the acidic sequence. Fig. 6*b* shows intracellular Ca^{2+} in response to stimulation with 0.1, 1, and 10 μM ATP. The most striking observation is that only cells expressing PEP-19 showed a robust increase in intracellular Ca^{2+} in response to 0.1 μM ATP. As summarized in Fig. 6*c*, control cells were unresponsive to 0.1 μM ATP, but 65% (35/54) of cells expressing PEP-19 responded with a significant increase in intracellular Ca^{2+} levels. Fig. 6*d* shows that peak intracellular Ca^{2+} release stimulated by 1 and 10 μM ATP was also significantly higher in cells expressing PEP-19 relative to control cells. Finally, Fig. 6*e* shows that PEP-19 increases the frequency of Ca^{2+} oscillations induced by 1 μM ATP relative to control cells.

In contrast to native PEP-19, Fig. 6*c* shows that only 5% of all cells expressing PEP(P37G), PEPscram, or PEPΔAc responded to 0.1 μM ATP with an increase in Ca^{2+}. Fig. 6*d* shows that peak Ca^{2+} levels induced by 1 and 10 μM ATP are also significantly lower in cells expressing mutant PEP(P37G), PEPscram, or PEPΔAc relative to PEP-19. Moreover, Fig. 6*d* shows the mutant PEP-19 proteins do not mimic the effect of native PEP-19 on Ca^{2+} oscillation frequency at 1 mM ATP. These data demonstrate that simply binding CaM is not sufficient and that the native acidic sequence in PEP-19 is required to sensitize HeLa cells to ATP-dependent Ca^{2+} release.

DISCUSSION

Cell signaling pathways must be regulated at multiple levels to control the amplitude and temporal characteristics of cellular responses and to prevent chaotic signaling that can lead to cell damage or death. Calmodulin is primarily regulated by intracellular Ca^{2+}, which is in turn controlled by cell-specific arrays of Ca^{2+} channels, pores, and pumps (27). A poorly understood regulatory mechanism involves the actions of dedicated regulators of CaM signaling, which have no known intrinsic activity other than binding to CaM. For example, the small neuronal phosphoprotein called ARPP-21, or regulator of calmodulin signaling, binds to Ca^{2+}-CaM to competitively inhibit activation of calcineurin and block suppression of L-type Ca^{2+} currents (28). PEP-19 is also a small protein with the potential to broadly affect CaM signaling by binding to apo- or Ca^{2+}-CaM via its IQ motif.

An obvious potential mechanism for PEP-19 is to competitively inhibit activation of CaM targets as proposed in the camstatin model (12). A caveat to this is that enzymes such as CaM kinase II bind CaM with 10,000-fold greater affinity than does PEP-19. Nevertheless, CaM binds to many proteins with low affinity, and PEP-19 would be particularly effective as an antag-

TABLE 2

Effect of ionic strength on Ca^{2+} binding to CaM

Apparent K_{Ca}, Hill coefficients, and k_{off} rates were determined as described under "Experimental Procedures." Values are the average ± S.D. of at least three experiments. The k_{on} was calculated from $k_{on} = k_{off}/KCa$. The buffer is 20 mM MOPS, pH 7.5, with the indicated concentration of KCl. An ionic strength of 13 mM is contributed by 20 mM MOPS at this pH. PEP-19 was added to a final concentration of 30 μM.

KCl	PEP-19	KCa	Hill coefficient	k_{off}	k_{on}
mM		*μM*		s^{-1}	$\mu M^{-1} s^{-1}$
100	−	1.6 ± 0.1	1.8 ± 0.1	12.5 ± 0.1	7.8
0	−	0.12 ± 0.01	1.8 ± 0.04	7.0 ± 0.2	58
100	+	2.0 ± 0.1	1.1 ± 0.01	428 ± 40	214
0	+	0.14 ± 0.01	1.0 ± 0.05	363 ± 24	2592

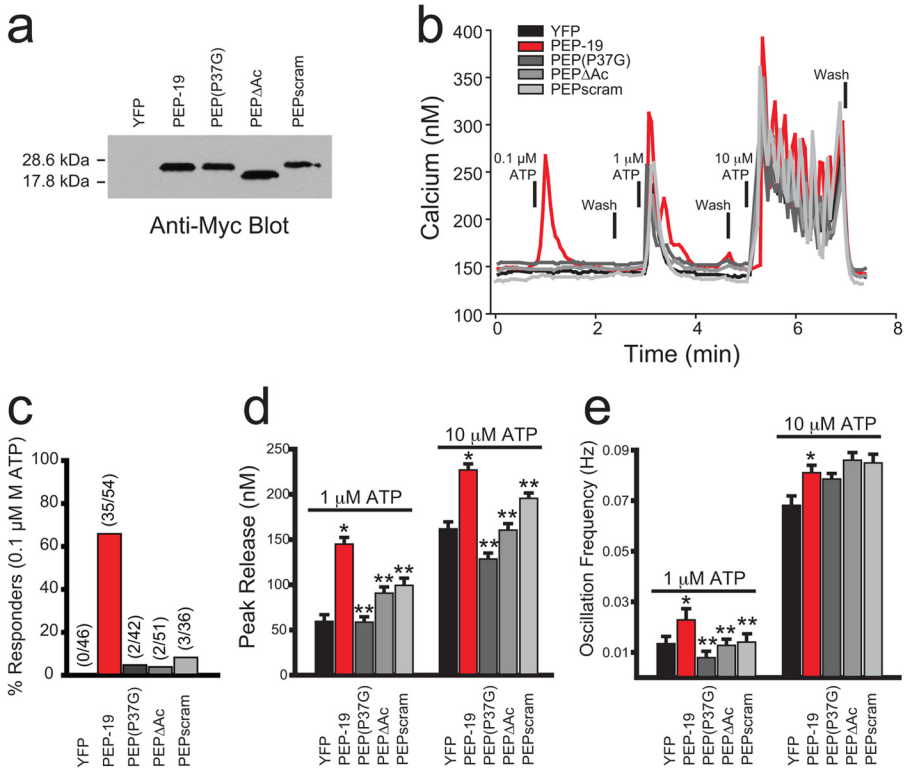

FIGURE 6. **Effect of PEP-19 and its derivatives on ATP-induced intracellular Ca^{2+} release.** Western blots in *a* show the relative level of expression of Myc-tagged PEP-19 and mutant proteins in HeLa cells that were transiently transfected with the corresponding expression plasmids. *b* shows intracellular Ca^{2+} levels in single cells in response to increasing concentrations of ATP. *c* shows the percentage of cells from each group that showed increased intracellular Ca^{2+} in response to 0.1 μM ATP. *d* and *e* show the effect of PEP-19 and mutated derivatives on peak Ca^{2+} levels and Ca^{2+} oscillation frequency, respectively, in response to 1 μM and 10 μM ATP. Data in *d* and *e* are represented as mean ± S.E. Statistical significance was determined with a Student's *t* test with * indicating $p < 0.05$ *versus* YFP and ** indicating $p < 0.05$ *versus* PEP-19.

onist of proteins that bind preferentially to the apo- or Ca^{2+}-bound C-domain of CaM. Another mechanism, the calpacitin model (14), proposes that higher affinity binding of PEP-19 to apo-CaM relative to Ca^{2+}-CaM retards its release during a Ca^{2+} pulse thereby affecting the temporal profile of available CaM and decreasing the overall rate of association of CaM with Ca^{2+}-dependent target proteins, especially at low Ca^{2+} levels. This model stems from early studies showing that the homologous protein, neuromodulin, binds preferentially to apo-CaM (29). However, this selectivity is only observed at low salt, and neuromodulin binds with equal affinity to apo- and Ca^{2+}-CaM in buffers containing 150 mM KCl (30). PEP-19 also has little selectivity for apo- *versus* Ca^{2+}-CaM at physiologically relevant concentrations of salt (12, 16).

These caveats to proposed mechanisms for PEP-19 led us to explore alternatives. We first showed that PEP-19 increased k_{on} and k_{off} rates for Ca^{2+} binding to the C-domain of CaM by 30–40-fold without greatly affecting K_{Ca} (15). Importantly, an acidic sequence located adjacent to the IQ motif is required for PEP-19 to modulate Ca^{2+} binding to CaM (16). Thus, PEP-19 has the potential to modulate the rate-limiting kinetics of Ca^{2+} binding to CaM and to provide a regulatory mechanism that is analogous to regulators of G-protein signaling, or RGS proteins, that modulates nucleotide hydrolysis (31).

The first goal of this study was to investigate the molecular mechanism of action of PEP-19. Our results show the following: 1) the native sequence of the acidic region as well as backbone constraints imposed by Pro-37 are required for PEP-19 to modulate Ca^{2+} binding to CaM; 2) the acidic sequence has weak Ca^{2+} binding properties. Interestingly, mutations that compromise the ability of PEP-19 to modulate Ca^{2+} binding to CaM have proportional effects on both k_{on} and k_{off} (see Table 1), which suggests that a similar mechanism is responsible, at least in part, for modulating both parameters. A role for acidic residues in tuning the Ca^{2+} k_{on} but not k_{off} for binding to Ca^{2+} EF-hand proteins was demonstrated by Martin *et al.* (32), who

showed that neutralizing three acidic surface residues near EF loop I in calbindin D9k decreased the k_{on} up to 50-fold. By analogy, the acidic sequence of PEP-19 may mimic an increase in negative surface charge near site III and/or IV of CaM, thereby increasing the Ca^{2+} k_{on} CaM by stabilizing a Ca^{2+}-CaM initiation complex or by electrostatically steering Ca^{2+} to sites III and/or IV. PEP-19 may increase the Ca^{2+} k_{off} of CaM by providing a low affinity transition Ca^{2+}-binding site that shuttles Ca^{2+} to the solvent rather than allowing it to rebind to the EF-hands of CaM. The inability of PEP(P37G) and PEPscram to modulate Ca^{2+} k_{on} and k_{off} may be due to repositioning the acidic residues relative to the EF-hand Ca^{2+}-binding loops in CaM and/or compromising Ca^{2+} binding to PEP-19.

The second goal of this study was to determine whether PEP-19 modulates CaM-dependent signaling pathways that affect intercellular Ca^{2+} homeostasis. We selected purinergic ATP-induced Ca^{2+} release as a model system because this pathway involves multiple potential points of regulation by CaM. The data in Fig. 6 show that PEP-19 sensitizes HeLa cells to ATP-dependent Ca^{2+} release and also alters the frequency of Ca^{2+} oscillations. Importantly, these biological effects require an intact acidic sequence, not simply binding of PEP-19 to CaM. Additional studies will be necessary to identify the level at which PEP-19 impacts Ca^{2+} release, but these effects reinforce the idea that both PEP-19 and Ng play roles in intercellular Ca^{2+} homeostasis (33). Such a role would be consistent with expression of PEP-19 in neuroendocrine and neuronal cells such as Purkinje cells (34) that have highly active Ca^{2+} signaling dynamics with robust and prolonged trains of action potentials (35). Ng knock-out mice show multiple effects on Ca^{2+} dynamics, including increased base-line Ca^{2+} levels and blunted Ca^{2+} transients induced by synaptic activity or glutamate receptor agonists (36). We anticipate PEP-19 and Ng will influence distinct sets of Ca^{2+} mobilization proteins and/or have different effects on the same proteins because PEP-19 increases both k_{on} and k_{off} of Ca^{2+} binding to the C-domain (15), whereas Ng increases only Ca^{2+} k_{off} leading to decreased Ca^{2+} binding affinity (37). Different cellular effects of PEP-19 and Ng are also suggested by different patterns of expression and because PEP-19 has anti-apoptotic effects (9, 10), whereas RC3 is reported to have pro-apoptotic activity (38, 39).

Calmodulin regulates numerous proteins involved in Ca^{2+} mobilization that could be tuned by PEP-19. With respect to ATP-dependent Ca^{2+} release, CaM directly and indirectly impacts phospholipase C activity (40), and it also modulates the activity of the IP_3 receptor (41) and store-operated Ca^{2+} entry channels (42) subsequent to IP_3 generation. Other CaM-dependent channels and extrusion proteins include the ryanodine receptor (43), plasma membrane Ca^{2+} pumps (44), and the Na^+/Ca^{2+} exchanger (45). Interestingly, the modes of interaction between CaM and several key Ca^{2+} mobilization proteins may make them particularly susceptible to PEP-19 because it binds selectively to the C-domain of CaM. For example, voltage-operated Ca^{2+} channels (46) and the IP_3 receptor (47) rely on selective, sequential, or stepwise interactions with the C-domain of CaM in its apo- or Ca^{2+}-bound forms.

In summary, this study reveals new mechanisms of action for PEP-19 and demonstrates novel effects on ATP-dependent Ca^{2+} release that do not depend solely on binding PEP-19 to CaM, but it also requires its ability to modulate Ca^{2+} binding to CaM. Tuning the activities of Ca^{2+} mobilization pathways would place PEP-19 at the top of CaM signaling cascades, with great potential to exert broad effects on downstream CaM targets, thus expanding the biological significance of this small regulator of CaM signaling.

REFERENCES

1. Ge, X., Yamamoto, S., Tsutsumi, S., Midorikawa, Y., Ihara, S., Wang, S. M., and Aburatani, H. (2005) Interpreting expression profiles of cancers by genome-wide survey of breadth of expression in normal tissues. *Genomics* **86,** 127–141
2. Sköld, K., Svensson, M., Nilsson, A., Zhang, X., Nydahl, K., Caprioli, R. M., Svenningsson, P., and Andrén, P. E. (2006) Decreased striatal levels of PEP-19 following MPTP lesion in the mouse. *J. Proteome Res.* **5,** 262–269
3. Iwamoto, K., Bundo, M., Yamamoto, M., Ozawa, H., Saito, T., and Kato, T. (2004) Decreased expression of NEFH and PCP4/PEP-19 in the prefrontal cortex of alcoholics. *Neurosci. Res.* **49,** 379–385
4. Glynne, R., Ghandour, G., Rayner, J., Mack, D. H., and Goodnow, C. C. (2000) B-lymphocyte quiescence, tolerance, and activation as viewed by global gene expression profiling on microarrays. *Immunol. Rev.* **176,** 216–246
5. Kanamori, T., Takakura, K., Mandai, M., Kariya, M., Fukuhara, K., Kusakari, T., Momma, C., Shime, H., Yagi, H., Konishi, M., Suzuki, A., Matsumura, N., Nanbu, K., Fujita, J., and Fujii, S. (2003) PEP-19 overexpression in human uterine leiomyoma. *Mol. Hum. Reprod.* **9,** 709–717
6. Wei, P., Blundon, J. A., Rong, Y., Zakharenko, S. S., and Morgan, J. I. (2011) Impaired locomotor learning and altered cerebellar synaptic plasticity in pep-19/PCP4-null mice. *Mol. Cell. Biol.* **31,** 2838–2844
7. Harashima, S., Wang, Y., Horiuchi, T., Seino, Y., and Inagaki, N. (2011) Purkinje cell protein 4 positively regulates neurite outgrowth and neurotransmitter release. *J. Neurosci. Res.* **89,** 1519–1530
8. Mouton-Liger, F., Thomas, S., Rattenbach, R., Magnol, L., Larigaldie, V., Ledru, A., Herault, Y., Verney, C., and Créau, N. (2011) PCP4 (PEP-19) overexpression induces premature neuronal differentiation associated with Ca^{2+}/calmodulin-dependent kinase II-δ activation in mouse models of Down syndrome. *J. Comp. Neurol.* **519,** 2779–2802
9. Erhardt, J. A., Legos, J. J., Johanson, R. A., Slemmon, J. R., and Wang, X. (2000) Expression of PEP-19 inhibits apoptosis in PC12 cells. *Neuroreport* **11,** 3719–3723
10. Kanazawa, Y., Makino, M., Morishima, Y., Yamada, K., Nabeshima, T., and Shirasaki, Y. (2008) Degradation of PEP-19, a calmodulin-binding protein, by calpain is implicated in neuronal cell death induced by intracellular Ca^{2+} overload. *Neuroscience* **154,** 473–481
11. Utal, A. K., Stopka, A. L., Roy, M., and Coleman, P. D. (1998) PEP-19 immunohistochemistry defines the basal ganglia and associated structures in the adult human brain and is dramatically reduced in Huntington's disease. *Neuroscience* **86,** 1055–1063
12. Slemmon, J. R., Morgan, J. I., Fullerton, S. M., Danho, W., Hilbush, B. S., and Wengenack, T. M. (1996) Camstatins are peptide antagonists of calmodulin based upon a conserved structural motif in PEP-19, neurogranin, and neuromodulin. *J. Biol. Chem.* **271,** 15911–15917
13. Gerendasy, D. D., Herron, S. R., Watson, J. B., and Sutcliffe, J. G. (1994) Mutational and biophysical studies suggest RC3/neurogranin regulates calmodulin availability. *J. Biol. Chem.* **269,** 22420–22426
14. Gerendasy, D. D., and Sutcliffe, J. G. (1997) RC3/neurogranin, a postsynaptic calpacitin for setting the response threshold to calcium influxes. *Mol. Neurobiol.* **15,** 131–163
15. Putkey, J. A., Kleerekoper, Q., Gaertner, T. R., and Waxham, M. N. (2003) A new role for IQ motif proteins in regulating calmodulin function. *J. Biol. Chem.* **278,** 49667–49670
16. Putkey, J. A., Waxham, M. N., Gaertner, T. R., Brewer, K. J., Goldsmith, M., Kubota, Y., and Kleerekoper, Q. K. (2008) Acidic/IQ motif regulator of calmodulin. *J. Biol. Chem.* **283,** 1401–1410
17. Xiong, L. W., Kleerekoper, Q. K., Wang, X., and Putkey, J. A. (2010) Intra- and interdomain effects due to mutation of calcium-binding sites in cal-

modulin. *J. Biol. Chem.* **285,** 8094–8103
18. Linse, S., Helmersson, A., and Forsén, S. (1991) Calcium binding to calmodulin and its globular domains. *J. Biol. Chem.* **266,** 8050–8054
19. Stieren, E., Werchan, W. P., El Ayadi, A., Li, F., and Boehning, D. (2010) FAD mutations in amyloid precursor protein do not directly perturb intracellular calcium homeostasis. *PLoS ONE* **5,** e11992
20. Wang, X., Kleerekoper, Q. K., Xiong, L. W., and Putkey, J. A. (2010) Intrinsically disordered PEP-19 confers unique dynamic properties to apo and calcium calmodulin. *Biochemistry* **49,** 10287–10297
21. Kleerekoper, Q. K., and Putkey, J. A. (2009) PEP-19, an intrinsically disordered regulator of calmodulin signaling. *J. Biol. Chem.* **284,** 7455–7464
22. Fallon, J. L., Halling, D. B., Hamilton, S. L., and Quiocho, F. A. (2005) Structure of calmodulin bound to the hydrophobic IQ domain of the cardiac Ca(v)1.2 calcium channel. *Structure* **13,** 1881–1886
23. Persechini, A., White, H. D., and Gansz, K. J. (1996) Different mechanisms for Ca^{2+} dissociation from complexes of calmodulin with nitric oxide synthase or myosin light chain kinase. *J. Biol. Chem.* **271,** 62–67
24. Xiong, L., Kleerekoper, Q. K., He, R., Putkey, J. A., and Hamilton, S. L. (2005) Sites on calmodulin that interact with the C-terminal tail of Cav1.2 channel. *J. Biol. Chem.* **280,** 7070–7079
25. Meador, W. E., Means, A. R., and Quiocho, F. A. (1993) Modulation of calmodulin plasticity in molecular recognition on the basis of x-ray structures. *Science* **262,** 1718–1721
26. Yang, W., Jones, L. M., Isley, L., Ye, Y., Lee, H. W., Wilkins, A., Liu, Z. R., Hellinga, H. W., Malchow, R., Ghazi, M., and Yang, J. J. (2003) Rational design of a calcium-binding protein. *J. Am. Chem. Soc.* **125,** 6165–6171
27. Berridge, M. J., Bootman, M. D., and Roderick, H. L. (2003) Calcium signaling. Dynamics, homeostasis, and remodeling. *Nat. Rev. Mol. Cell Biol.* **4,** 517–529
28. Rakhilin, S. V., Olson, P. A., Nishi, A., Starkova, N. N., Fienberg, A. A., Nairn, A. C., Surmeier, D. J., Greengard, P. (2004) A network of control mediated by regulator of calcium/calmodulin-dependent signaling. *Science* **306,** 698–701
29. Andreasen, T. J., Luetje, C. W., Heideman, W., and Storm, D. R. (1983) Purification of a novel calmodulin binding protein from bovine cerebral cortex membranes. *Biochemistry* **22,** 4615–4618
30. Alexander, K. A., Cimler, B. M., Meier, K. E., and Storm, D. R. (1987) Regulation of calmodulin binding to P-57. A neurospecific calmodulin-binding protein. *J. Biol. Chem.* **262,** 6108–6113
31. Xie, G. X., and Palmer, P. P. (2007) How regulators of G protein signaling achieve selective regulation. *J. Mol. Biol.* **366,** 349–365
32. Martin, S. R., Linse, S., Johansson, C., Bayley, P. M., and Forsén, S. (1990) Protein surface charges and Ca^{2+} binding to individual sites in calbindin D9k. Stopped-flow studies. *Biochemistry* **29,** 4188–4193
33. Slemmon, J. R., Feng, B., and Erhardt, J. A. (2000) Small proteins that modulate calmodulin-dependent signal transduction: effects of PEP-19, neuromodulin, and neurogranin on enzyme activation and cellular homeostasis. *Mol. Neurobiol.* **22,** 99–113
34. Ziai, M. R., Sangameswaran, L., Hempstead, J. L., Danho, W., and Morgan, J. I. (1988) An immunochemical analysis of the distribution of a brain-specific polypeptide, PEP-19. *J. Neurochem.* **51,** 1771–1776
35. Hartmann, J., and Konnerth, A. (2005) Determinants of postsynaptic Ca^{2+} signaling in Purkinje neurons. *Cell Calcium* **37,** 459–466
36. van Dalen, J. J., Gerendasy, D. D., de Graan, P. N., Schrama, L. H., and Gruol, D. L. (2003) Calcium dynamics are altered in cortical neurons lacking the calmodulin-binding protein RC3. *Eur. J. Neurosci.* **18,** 13–22
37. Gaertner, T. R., Putkey, J. A., and Waxham, M. N. (2004) RC3/neurogranin and Ca^{2+}/calmodulin-dependent protein kinase II produce opposing effects on the affinity of calmodulin for calcium. *J. Biol. Chem.* **279,** 39374–39382
38. Devireddy, L. R., and Green, M. R. (2003) Transcriptional program of apoptosis induction following interleukin 2 deprivation. Identification of RC3, a calcium/calmodulin-binding protein, as a novel proapoptotic factor. *Mol. Cell. Biol.* **23,** 4532–4541
39. Gui, J., Song, Y., Han, N. L., and Sheu, F. S. (2007) Characterization of transcriptional regulation of neurogranin by nitric oxide and the role of neurogranin in SNP-induced cell death. Implication of neurogranin in an increased neuronal susceptibility to oxidative stress. *Int. J. Biol. Sci.* **3,** 212–224
40. McCullar, J. S., Larsen, S. A., Millimaki, R. A., and Filtz, T. M. (2003) Calmodulin is a phospholipase C-β interacting protein. *J. Biol. Chem.* **278,** 33708–33713
41. Taylor, C. W., and Laude, A. J. (2002) IP3 receptors and their regulation by calmodulin and cytosolic Ca^{2+}. *Cell Calcium* **32,** 321–334
42. Zhu, M. X. (2005) Multiple roles of calmodulin and other Ca^{2+}-binding proteins in the functional regulation of TRP channels. *Pflugers Arch.* **451,** 105–115
43. Rodney, G. G., Williams, B. Y., Strasburg, G. M., Beckingham, K., and Hamilton, S. L. (2000) Regulation of RYR1 activity by Ca^{2+} and calmodulin. *Biochemistry* **39,** 7807–7812
44. Di Leva, F., Domi, T., Fedrizzi, L., Lim, D., and Carafoli, E. (2008) The plasma membrane Ca^{2+}-ATPase of animal cells. Structure, function and regulation. *Arch. Biochem. Biophys.* **476,** 65–74
45. Carafoli, E., and Longoni, S. (1987) The plasma membrane in the control of the signaling function of calcium. *Soc. Gen. Physiol. Ser.* **42,** 21–29
46. Liang, H., DeMaria, C. D., Erickson, M. G., Mori, M. X., Alseikhan, B. A., and Yue, D. T. (2003) Unified mechanisms of Ca^{2+} regulation across the Ca^{2+} channel family. *Neuron* **39,** 951–960
47. Kang, S., Kwon, H., Wen, H., Song, Y., Frueh, D., Ahn, H. C., Yoo, S. H., Wagner, G., and Park, S. (2011) Global dynamic conformational changes in the suppressor domain of IP3 receptor by stepwise binding of the two lobes of calmodulin. *FASEB J.* **25,** 840–850